Standard Target Calibration of Broad-Band Active Sonar Systems in a Laboratory Tank

A. Islas-Cital, P.R. Atkins, K.Y. Foo
The University of Birmingham
School of Engineering
Electronic, Electrical and Computer Engineering

Abstract-**High-frequency, scientific active sonar systems are frequently calibrated using standard target spheres. Spot frequency calibration accuracies (using carefully optimized sphere diameters) of 0.1 dB have been previously established as theoretically and technically feasible. The premise of this work is that a tungsten-carbide sphere may be used to calibrate an arbitrary sonar system in a laboratory water tank. In order to achieve an accurate calibration it is necessary to obtain exact knowledge of the characteristics of the immersion medium and the target. With this aim, the temperature and salinity of the water was accurately determined, resulting in an estimate of the sound speed of the water. The density and composition of the spheres were examined using laboratory equipment. Moreover, various other sources of variability have been addressed. For the purposes of this work, seven tungsten carbide spheres of different sizes were used to perform inter-comparison calibration estimates. Measured and modeled target strength curves were compared across the bandwidth of 50 to 150 kHz. Comparative results are presented for all the spheres, with the best-case average precision of 0.22 dB being obtained for the 25 mm sphere.**

I. Introduction

Spherical standard targets for the calibration of sonar systems are well-established, especially for applications in the field of oceanography and fisheries. Mainly due to the work of Foote [1][2][3], this method has been refined for on-vessel calibrations, with copper or tungsten carbide spheres, and a potential accuracy of 0.1 dB. In practice, the achievement of such a high level of precision is dependent on the exact knowledge of target properties and medium conditions, the relative proximity of resonances in the band of interest, and the joint effects of multiple other factors (reverberation, multipath, equipment stability, target location within the beam, etc).

The procedure involves insonifying a sphere deployed underneath the vessel by means of a hull-mounted echo sounder. Deconvolving the modeled form function of that target from the received scattered pressure yields the complete system response for the relevant bandwidth. Traditionally, the calibration is performed at the spot-frequencies at which standard echo-sounders in fisheries operate, for example, 38 and 120 kHz. Therefore, the minimization of errors by optimizing the sphere diameters has been focused on these individual frequencies, and accordingly the accuracies quoted often refer only to narrow-band calibration procedures.

In the case of broadband calibration procedures, the elastic resonances of the target, present as prominent features in the form function, have to be considered. Due to the accentuated changes of phase and amplitude in the vicinity of these resonances, significant calibration inaccuracies will be introduced and it is preferable to avoid these frequency regions for calibration purposes. Nevertheless, resonances are bound to appear in wide-bandwidth calibration procedures. To address this issue, it has been proposed that multiple spheres be used simultaneously, in a way that their juxtaposition eliminates the nulls [4]. But since this scheme increases logistic complexity, other approaches have been explored, such as resolving the front interface echo (or rigid reflection), which does not depend on frequency so strongly [5][6].

In this paper, the elastic effects of the tungsten carbide spheres are examined through the analysis of their material properties, namely density and bulk speeds, which are in-turn influenced by the amount of cobalt binder present [7]. It is known that deviations from manufacturer's specifications or published values will thus result in deviations in calibration [8].

Studies of a similar nature as this one have been carried out in the past [2]. However, the majority of them have been oriented at traditional sonar systems for fisheries, and therefore parameters are varied around their specific operating conditions. However, two investigations of the calibration of the same scientific multibeam sonar, do examine a bandwidth from 65 to 125 kHz [8][9]. It is our intention to continue this type of investigation, and to carry out a survey of some of the uncertainties and challenges entailed in the standard-target calibration method, for a broad-band generic sonar in a laboratory tank setting. Also, in a broader sense and without necessarily being tied to sonar calibration, it is believed that the backscattering measurements on spheres in laboratory tanks has a continued scientific relevance, thus justifying the need for an overview of the experimental conditions that might be encountered.

Nowadays, laboratory tanks remain a valuable tool in underwater acoustics. For example, in spite of the impact of reverberation and the detrimental effect upon accuracy, the calibration of practical sonar systems in laboratory tanks is viable, and is sometimes performed prior to field deployment [10]. Furthermore, due to their potential for generalization and the advantage of controlled conditions, experiments with spheres in laboratory water tanks often function as benchmark for an assortment of field applications. Recently for example, NURC has used fiberglass spherical shells in a

978-1-4244-5222-4/10/$26.00 ©2010 IEEE

tank to assess methods for structural health monitoring [11], while in Japan tungsten carbide spheres served to evaluate a target identification scheme based on dolphin-like signals [12].

II. EXPERIMENTAL METHOD AND EQUIPMENT

Acoustic backscattering measurements were conducted within the water tank laboratory of the University of Birmingham, a concrete facility with dimensions 8.49 m, 3.95 m and 3.04 m. The targets were suspended on a X-Y table for fine positioning. To ameliorate the strength of multi-paths and reverberation, the transducer and the targets were located at mid-depth, at the mid-point between the side walls and at 1/3 and 2/3 of the length, respectively. The whole arrangement is illustrated in Fig.1.

A)

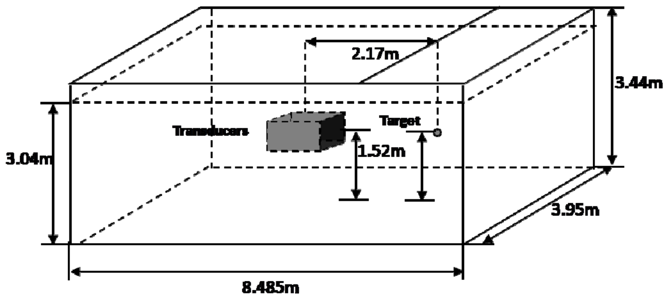

B)

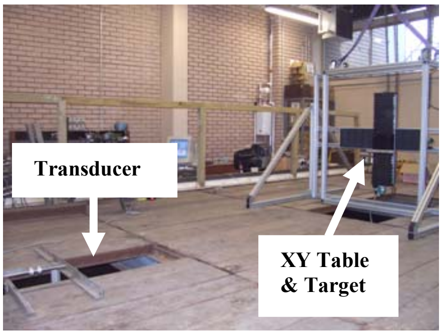

Figure 1.
A) Schematic location of transducer and targets in the tank.
B) Laboratory tank, with transducer frame and X-Y table shown.

A single piezoelectric transducer was used as both transmitter and receiver. The chosen transducer was a Reson TC2130 with a central frequency of 100 kHz, and maximum hydrophone and projector sensitivities at 104 kHz of -182.04 dB re 1V/µPa and 157.32 dB re µPa/1V, respectively.

A data acquisition card converted the transmit pulses generated in Matlab into analog waveforms, and digitized the received backscattered echoes. It also provided the control signals necessary to switch between transmit and receive modes. The interface equipment was the National Instruments M-series 6251 model, which has eight differential 16-bit analog inputs, with a sampling rate of 1.25 MS/s on a single-channel, two 16-bit analog outputs, and twenty four digital I/Os. Transmit amplifier, low-pass filters, RX/TX switch and differential receiver amplifier were custom-made for this experiment.

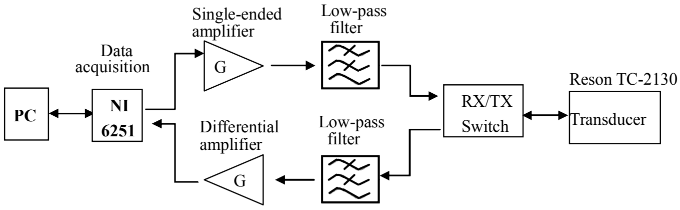

Figure 2. Schematic electrical system.

The tungsten carbide spheres deployed in this experiment were manufactured by Spheric Trafalgar Ltd., with a dimensional tolerance of ±0.35 µm, 6 of them with cobalt binder (nominal content: 5 - 7%) and 1 with nickel binder (nominal content 8 - 10%).

The extraction of an empirical form function was carried out in two stages. First, a sphere without resonances in the relevant bandwidth, was used to obtain the complete system response. The measured backscattered pressure was averaged and recorded for 100 Hz frequency steps, and the predicted form function was deconvolved from the measured data. Then, a second sphere was placed into the tank for backscattering measurements. Deconvolving the system response from the measured data yielded the experimental form function. Both curves where then expressed as logarithmic target strength values. In our case, the system response was always that obtained from the 20 mm diameter sphere.

III. SOURCES OF ERROR

The factors affecting the agreement between measured and predicted form function curves and, implicitly, calibration accuracy, were divided in three groups: a) System and operational variability, b) Immersion medium variability and c) Target variability. The following paragraphs will briefly explore each of these sections.

A. System and operational variability

These sources of error are to be found within the system itself, originating from limitations in bandwidth, resolution or degrees of instability. Also, perturbations caused during the process, such as reverberation, or random inconsistencies in the procedure, such as target suspension differences, are also included.

Target position in acoustic beam

With the aim of attaining normal incidence and backscattering conditions, the target was placed in the centre of the transducer acoustic beam. From the directivity characteristics of the transducer it follows that deviating from the transducer axis will affect the amplitude of the received voltage. Moreover, it has been determined that the alignment angle and the transducer aperture size are factors that play an important role not only in the amplitude, but also in the phase of the scattered echo [13].

The centering of the target with respect to the transducer can be achieved by careful mechanical or optical alignment as exemplified by Neubauer *et al.* [14]. However, this does not account for any possible beam-squint within the transducer. Therefore, the directional properties of the complete system, the "effective" (also called "system") directivity characteristics [15] were obtained by moving a target across the acoustic field, delineating a three dimensional shape as a function of position and echo strength. This ensures that the artifacts of the equipment are taken into account in when the beam is profiled, and has been adopted to find out the transducer beam pattern in other works, such as [16]. A 3-D visualization of the profiling determined in this manner is shown in Fig. 3.

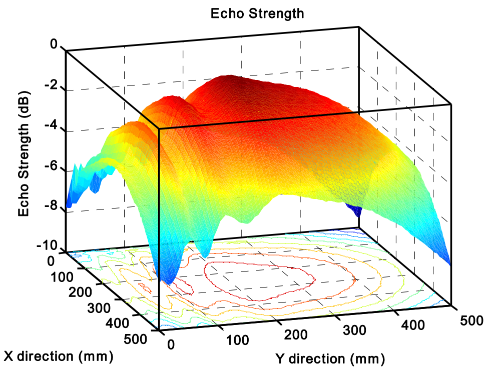

Figure 3. Acoustic beam profile.

The spheres were suspended on a 0.18 mm diameter braided fishing line made from aramid fibers, which exhibit minimum stretch, thus ensuring stable position. This was a substantial improvement upon nylon monofilament line, whose length was observed to change as much as 18 mm during and after submersion, probably due to water adsorption. To maintain strict consistency in string length among the different spheres and test runs, it was verified before every run and adjusted with a stay adjuster, as illustrated in Fig. 4.

Figure 4. Target suspension rig mounted on the X-Y table.

Reverberation

A crucial phenomenon of room acoustics, also relevant to test tanks, is the sound field formed by the multiplicity of echoes reflected from its boundaries. To minimize multipath interference, or masking, of the direct-path echo, the transducer was shielded from the ensuing reverberated field by enclosing it in a frame padded with acoustic absorbing material, as shown in Fig. 5.

Figure 5. Transducer encased in acoustic absorbing material.

Although a significant reduction was observed, a small level of reverberation remained, as Fig. 6 indicates, its impact upon calibration is frequency dependent.

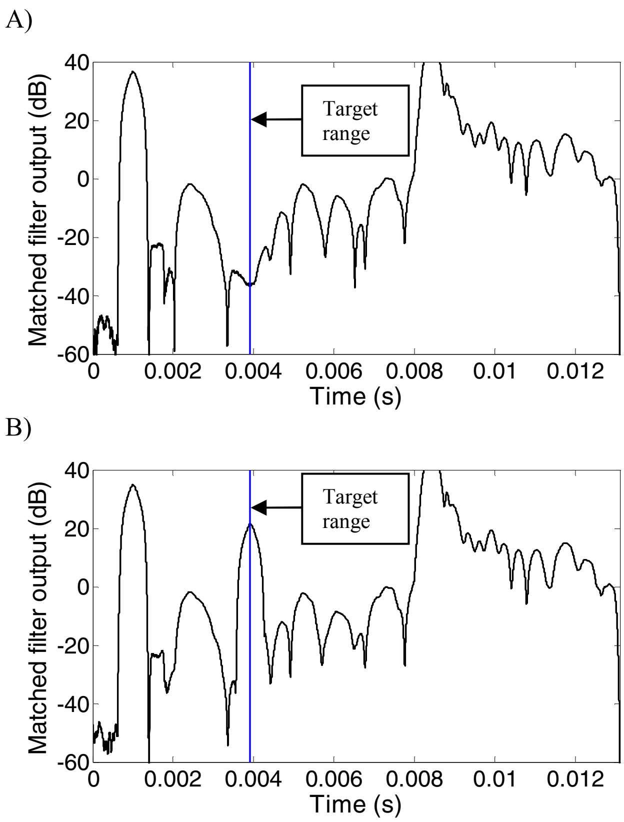

Figure 6. Reverberating conditions at target range.
A) Target not present
B) Target present

Electric noise and system stability

As is the case in most measurement exercises, the precision achieved in a task is ultimately limited by the resolution, accuracy and stability of the instrument itself. For a sonar, this comprises the transducer and independent linear devices such as the filters and amplifiers. In practice, ambient conditions, power source fluctuations or gain drifts can shift the output significantly, especially when signals are close to the noise floor. Such errors can skew a calibration outside the desired tolerance, and large discrepancies can be ascribed to stability problems [16].

To address this issue, a series of broad-band continuous measurements were conducted. First, to assess the levels and nature of noise, records were taken without a transmit signal being sent. It can be seen in Fig. 7 that the noise floor lies on top of a small negative DC offset, arising from marginal unbalance of the differential channels. This plot shows the Gaussian distribution fit to the typical measured system noise, exhibiting a mean of -8.3 mV and a standard deviation of 3.03 mV (in in an 300 kHz passive sonar bandwidth).

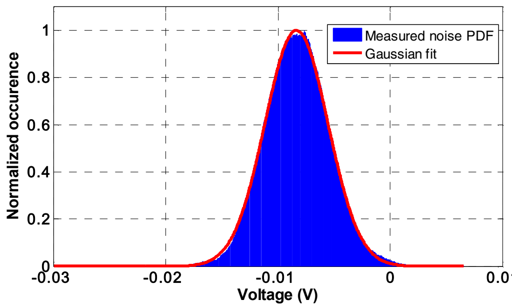

Figure 7. Passive sonar receive noise distribution with Gaussian fit

Secondly, the echo strength was recorded by pinging repeatedly at a fixed target over an extended period of time, windowing the echo time series and taking the absolute value of the Fourier transform at the frequency bin corresponded to the transmitter center frequency. Stability tests of the same character were also performed in [17] and [18]. One thousand pings, transmitted at a rate of one per minute, were impinged upon the 20 mm sphere and, as illustrated in Fig 8, the range of variation was in the order of 0.1 dB. With a standard deviation of 0.01 dB, this system demonstrated acceptable stability during the course of the experiment.

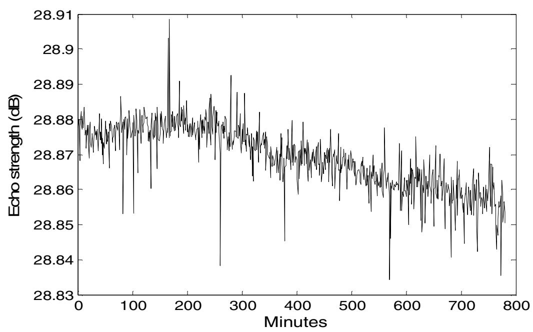

Figure 8. Ping-to-ping stability measurements.

Deviations from modeling assumptions

The applicability of theoretical predictions of backscattering from spheres rely on a number of premises. Namely, the particular set of expressions that we implemented, from the work of Goodman and Stern [19] is valid for steady-state, harmonic plane waves, such as found in the far-field range. In this respect, the actual distance between the target and the transducer active element, approximately 2.17 m, is well beyond the rule-of-thumb of 10 sphere diameters separation that fulfills the model's assumption [14].

The monostatic transmitted pulse length, 0.4 ms (corresponding to 0.6 m in the water), was long enough to ensure steady-state conditions and the frequency was stepped to comprise a total bandwidth from 50 to 150 kHz. This wavelength more than meets Hampton and McKinney's criteria that it must be longer than two sphere diameters [20]. However, this is not a perfect match to the target strength obtained with the infinite pulse length needed for true steady-state conditions, as noted in [21].

Additional operational factors

Various other potential sources of error are often invoked to address fractional inaccuracies not ascribed to known sources. For example, the random contribution of the supporting nets and possible surface contamination have been suggested as causes for variations in the measured echo strength values [22]. However, in terms of the main contributors to echo formation, the minute impact of the net on the backscattering can be disregarded due to its low target strength and the fact that when stretched over the sphere it presents a rather diffuse target, as demonstrated in [23]. Further confirmation of this assumption can be found in the work of Welsby and Goddard, who investigated and compared the effects of various sphere supporting schemes, arriving to the conclusion that the presence of bubbles on the material can be more influential in modifying the target strength [24]. Although it may be useful to explore the alternative method of fixing the string to the object with resin drops, the possible presence of bubbles should not be ignored.

Finally, the chance of spurious acoustic noise signals finding their way into the receiver is always possible, This is especially true for marine *in-situ* calibrations, where interference from biological activity have suggested the need for isolating the calibration site with a net [16].

B. Immersion medium variability

The characteristics of the surrounding medium determine the propagation of sound and, consequently, influence target strength. This is taken into account in the backscattering model through the parameters of density and sound speed. However, as Foote [2] points out, these values depend on the conditions of the medium, namely salinity, temperature, pressure, and should not be considered as independent variables [2]. Target strength variations induced by the medium will now be analyzed in terms of the prevailing physical properties of water in the laboratory tank.

Salinity

Salinity, expressed in grams/liter (g/l) or parts per thousand (ppt), can be defined as the level of "saltiness", or amount of salts dissolved in a given volume of water, or more precisely, the inorganic matter without halogens in 1 kg of water [25]. This quantity, whose fluctuations are subject to a complex interaction of natural and artificial processes, is one of the main descriptors in hydrology. The tap water filling the tank can be classified as "fresh," since it falls in the salinity range of rivers, streams and some lakes.

Salinity can be estimated from Total Dissolved Solids (TDS), since they are closely related indicators of the constituents of water. These figures, in turn, can be determined from electrical conductivity (EC), but due to composition uncertainties, conversion factors between them cannot be generalized and remain approximate. Both TDS and EC measurements were conducted, the former by a gravimetrical method involves weighting the solid residue after evaporation, and the latter with a Mettler Toledo S30 meter (accuracy of ±0.5%), arriving to a value of 0.11 ppt.

Temperature

For the present study a platinum resistor sensor connected to a TMS Europe Tracker 220 series indicator was used, with a reported uncertainty of ±0.075 °C. It was expected that the large volume contained in the tank (over 100,000 liters) restricted and slowed down temperature changes, rendering the thermal properties relatively constant. For the typical time scale of a single test this holds true, since the range and standard deviation over the course of even several hours can be considered negligible (σ=0.014°C), as evidenced by Fig. 9.

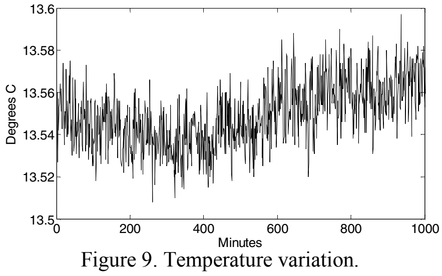

Figure 9. Temperature variation.
Range: 0.089 °C, Standard deviation: 0.014°C

Even if unlikely because of limited depth, temperature gradients may be significant and thus the temperature profiling of the tank was performed, as shown in Fig. 10.

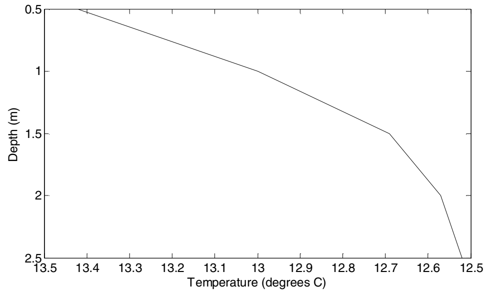

Figure 10. Temperature profile

Natural mixing processes such as storms are known to temporarily reduce temperature gradients in the ocean [26], in the same manner, pump circulation in the tank could be expected to improve the isothermal assumption.

Sound speed

The velocity of sound waves in water has a strong effect on the backscattering form function, and it is known that part of the inaccuracies of sonar calibration can be ascribed to errors in the estimation of this value [27]. In fact, in a similar error analysis study, Miyanohana *et al.*. only varied this parameter on the grounds of its impact upon target strength and inevitable uncertainties in determination [27].

In order to calculate sound speed as a function of our independent variables, salinity and temperature, an expression that relates these quantities is needed. The two equations with the most widespread acceptance are that of Del Grosso [28] and the UNESCO equation [29], based on the work of Chen and Millero [30], both of which allow for applicability in intermediate salinities. Recently, the UNESCO equation has been corrected in its lower salinity region by Leroy *et al.*. [30], producing a "merged equation" with the pure water formula of Belogol'skii *et al.* [32]. For the minimal depth of targets in the laboratory tank only slight divergences between Del Grosso's and the corrected UNESCO equation are to be expected, because they only start to deviate at higher pressures. These two equations were incorporated by [31] in a single expression.

Another viable option for the speed of sound in fresh water comes from Chen and Millero, who stressed the particularities of lakes, discouraging the assumption of pure water as an accurate representation of their pressure, volume and temperature properties [33]. They developed an equation of state applicable for the limnological range, that is, 0 - 0.6 ppt salinity, 0° - 30 °C, and 0- 180 bar [34]. The speed of sound calculated with these two equations was very similar. We have chosen to use the expression from Leroy *et al.* for all sound velocity calculations subsequently carried out.

Effects on acoustic target strength

Variations of salinity from the determined value of 0.11 ppt across the likely range in the tank (0.09 to 0.13 ppt), were found to have a negligible impact on target strength. At this salinity, sound speed and target strength are shown as a function of temperature in Fig. 11 and Fig. 12.

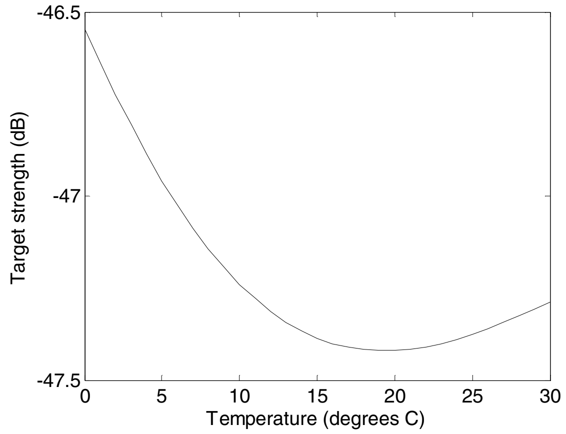

Figure 11. Temperature effects on target strength (Sphere diameter = 20mm, Frequency = 100 kHz, Salinity = 0.11 ppt)

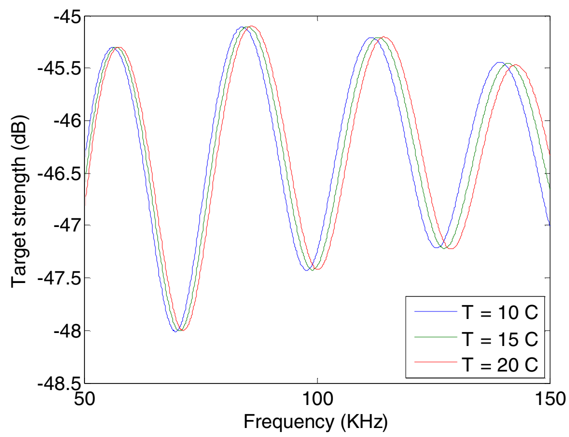

Figure 12. Temperature effects on target strength, full bandwidth (Sphere diameter = 20mm, Salinity = 0.11 ppt)

It can be noted that the complete temperature range encompasses nearly 1 dB variation, however, within the likely temperatures found in water tank (12 to 17 °C), this amplitude variation will be much less.

C. Target variability

It is well-known that the material properties of metallic spheres, such as their density, and transverse and longitudinal wave speeds, largely determine the shape of their backscattering form function. Particularly, they dominate the strong elastic or mechanical response that manifests as a series of deep nulls along the frequency axis, and therefore it becomes crucial to know the material properties with precision. The density was calculated from the mass measured in a Sartorius A 210P electronic scale, which reports a standard deviation of ±0.0001 gr. The results are shown in Table I.

TABLE I
MEASURED DENSITIES

Sphere Diameter	Density (kg/m^3)
20mm (A)	14932
20mm (B)	14963
22mm	14930
22mm (Ni)	14989
25mm	14861
30mm	14925
40mm	14907
50mm	14892

The mean value of the measured densities (14925 kg/m^3) stands slightly above the nominal value (for cobalt binder) most frequently cited in the literature, 14900 kg/m^3, obtained by [7] along with bulk velocities, from the exact localization of mechanical resonances through acoustic means. Variations in manufacturing, however, undermine the applicability of these values, especially through uncertainties in cobalt content. Cobalt, used as a binder in the sintering process, is known to alter the elasticity of tungsten carbide [7] and for this reason it was deemed useful to obtain a more precise value within its 5 - 7% stated tolerance. For this purpose, spectroscopic elemental analysis was performed with a Philips XL 30 Scanning Electron Microscope (SEM).

In the first SEM scanning, no traces of cobalt were detected in some of the spheres, namely the ones that had been most extensively used in the tank. It became clear that cobalt leaching phenomenon had occurred, due to prolonged exposure to the slightly chlorinated water of the laboratory tank. Even though tungsten carbide is more impervious to corrosion than other alloys, it is still vulnerable to cumulative attack by corrosive liquids [35].

This was verified in two ways, first, the 40 mm sphere, that previously had showed 4.29% cobalt, was submerged in the tank for approximately 90 hours. Afterwards, a second SEM experiment provided evidence of an unequivocal decrease to 2.48% (standard deviation 0.29%). Secondly, one of the spheres that originally presented no cobalt on the surface was cut, as pictured in Fig. 13, and its interior observed with the microscope.

Figure 13. Cut hemisphere of 20mm (A) TC sphere

Confirmation was found in the cut surface of one hemispheres, with 5.39 cobalt percentage and, moreover, it was established that the cobalt percentage clearly diminishes nearer the edge.

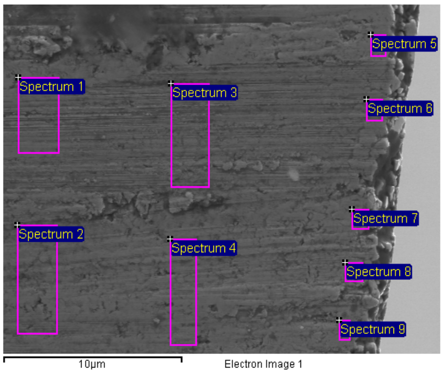

Figure 14. SEM image of cut hemisphere with cobalt content gradient

These findings made the use of tungsten carbide spheres with nickel binder attractive, due to their superior corrosion resistance [36]. A 22 mm tungsten carbide sphere with nickel binder was measured for density and composition, as well as acoustic backscattering.

Since cobalt leaching appears to be very superficial, a significant change on the overall properties of the sphere is not likely. Also, since it happens on the granular level, it would appear improbable that it influences acoustic scattering. However, the existence of an alternative more suitable for the corrosive conditions of the sea is noted.

The unreliability associated with merely examining the surface for cobalt content limited the usefulness of SEM analysis for our purposes. In addition to the cut 20 mm (A), we present results for surface SEM analysis of two spheres prior to their use in the tank.

TABLE II
SEM RESULTS: BINDER CONTENT

Sphere diameter	Content percentage
20 mm (A)	6.39 % cobalt
22 mm Co	5.81 % cobalt
22 mm Ni	5.39 % nickel

IV. SUMMARY AND RESULTS

Experimental conditions for conducting sonar calibration with standard spheres in a fresh water laboratory tank have been reviewed and the settings and equipment implemented for this task described. A survey of factors degrading the accuracy of calibration has been carried out.

Methods adopted for centering the target and combating reverberation have been discussed while possible discrepancies of real conditions with assumptions of the backscattering model have been addressed. Stability and noise checks were satisfactory, however, it is advisable to regularly confirm system performance parameters. Immersion medium parameters, namely temperature and salinity, displayed high stability, thus playing a lesser role in the results of this analysis.

Agreement between modeled and measured TS values was compared from 50 to 150 kHz bandwidth, using 7 tungsten carbide spheres. One of them, referred as 20 mm A, was only used for the extraction of the system response.

The accurate measurement of density of tungsten carbide spheres was useful in reducing the calibration error. The incorporation of the actual density values, instead of nominal ones, showed a marginal improvement in agreement between the measured and predicted form functions. However, it allows the approximation of shear and longitudinal wave speeds. Material properties were measured with SEM spectroscopy. Analysis showed some correlation between cobalt content and material density, partially in agreement with the data provided in [37]. However, reliable measures of cobalt content were elusive, in view of the inadequacies of our samples (convex, unpolished surfaces). It was conclusively proven that the prolonged exposure of spheres with cobalt binder to the water in the tank causes a complete leaching out of the cobalt from the surface. Therefore, a sphere with nickel binder, more resistant to corrosion, was included for tentative analysis of potential advantages as a target.

Fig. 15 displays the TS values, extracted experimentally over the 50 to 150 kHz bandwidth, along with the theoretical curve as derived in [19]. The level of mismatch, measured in terms of the absolute difference, is shown. The resulting agreement was relatively good. Differences over the entire band had an absolute mean value of under 1 dB, except for the larger sphere. In some cases, disagreement in the lower frequencies is caused by low SNR due to reduced sensitivity of the transducer. The error between measured and predicted form functions increases with sphere diameter due to the inclusion of more resonances. A second indicator of agreement was the RMS error of the measured and modeled form functions. The RMS error ranged from 0.03 to 0.17, comparing well with figures presented in [12].

The results indicate that it is challenging to obtain the potential broad-band accuracy of 0.1 dB as described in the literature for narrowband systems, though in every sphere we were able to achieve such precision within smaller sub-bands. This again adds evidence to the feasibility of using arbitrary tungsten carbide spheres for the calibration of sonar systems operating at specific frequencies.

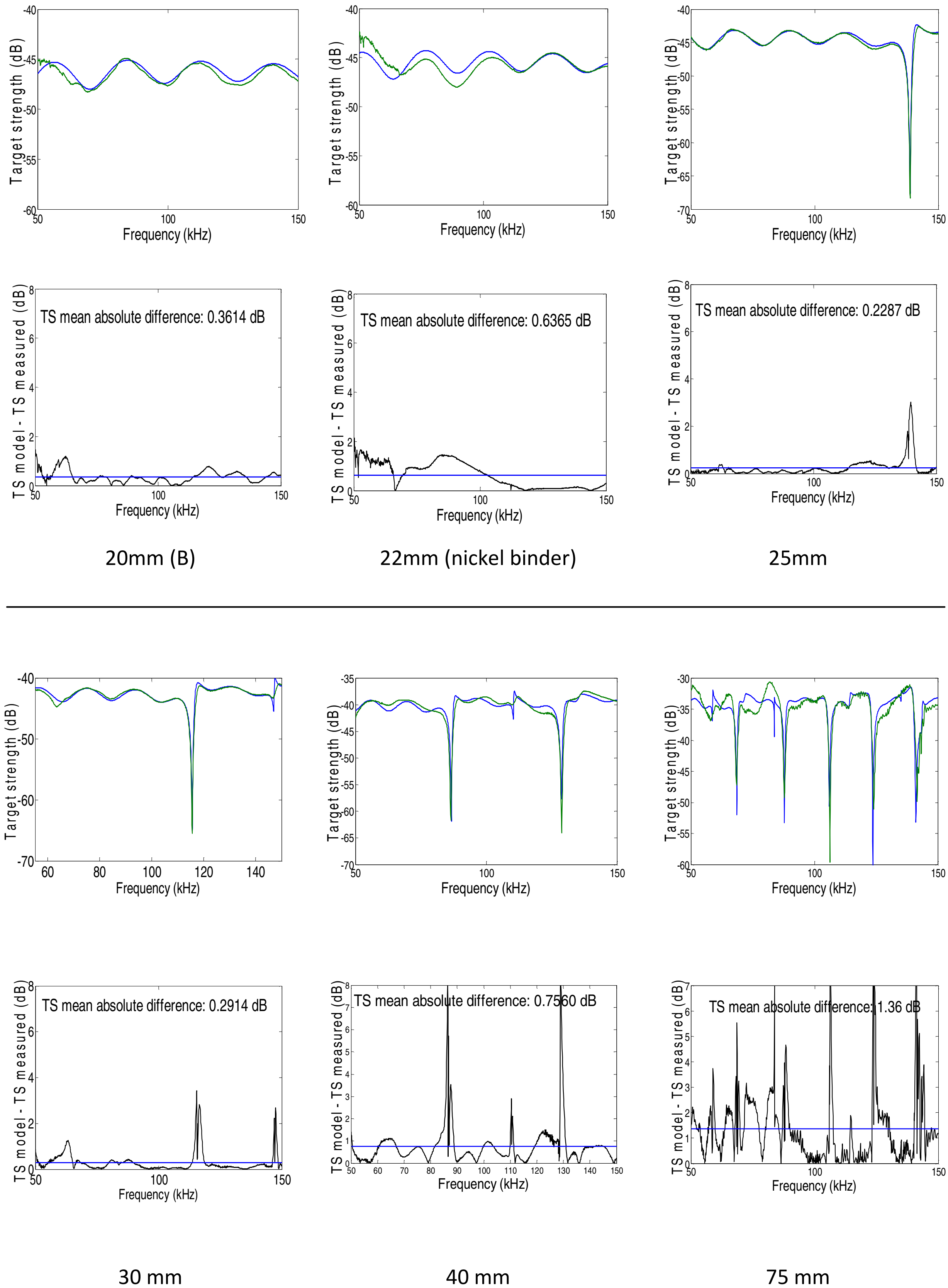

Figure 15. Modelled and measured TS curves
(Sphere diameter below each panel, line corresponds to mean absolute difference.)

V. CONCLUSIONS

We have reviewed all significant factors affecting accuracy of standard-target sonar calibration, carried out in a laboratory tank. In this environment the immersion medium parameters are highly stable, therefore, the main sources of variability are most likely to be found in the system or experimental settings.

After taking into account the large multiplicity of potential sources of error that can, independently or jointly, sway the accuracy away from its optimal value, we arrived to a calibration precision of 0.22 dB for a 25 mm diameter tungsten carbide sphere with cobalt binder, across the bandwidth of 50 to 150 kHz. For the rest of the spheres, an overall broadband calibration performance averaging 0.6 dB was demonstrated.

The remaining level of discrepancy be found in the system or experimental settings. The formation of gas bubbles on the target support is difficult to compensate, and is likely to have contributed to the mismatch in the calibration result..

ACKNOWLEDGMENT

We would like to thank Ms. Yina Guo and Mr. Paul Stanley, from Met & Mat, University of Birmingham, for the ESEM measurements presented here. Also, Ms. Monica Jaime, from Chemical Eng. University of Birmingham, is thanked for her help with TDS and density measurements.

REFERENCES

[1] Foote, K.G., (1982). Optimizing copper spheres for precision calibration of hydroacoustic equipment. *J. Acoust. Soc. Am.*, 71(3), pp. 742-747.

[2] Foote, K. G. (1983). Maintaining precision calibrations with optimal copper spheres. *J. Acoust. Soc. Am. , 73* (3), 1054-1063.

[3] Foote, K. G., & MacLennan, D. N. (1984). Comparison of copper and tungsten carbide calibration spheres. *J. Acoust. Soc. Am. , 75* (2), 612-616.

[4] Atkins, P. R., Francis, D., & Foote, K. G. (2008). Calibration of broadband sonar systems using multiple standard targets. *Acoustics 08 Conference Proceedings* , (pp. 2821-2826).

[5] Dragonette, L. R., Numrich, S. K., & Frank, L. J. (1981). Calibration technique for acoustic scattering measurements. *J.Acoust.Soc.Am. , 69* (4), 1186-1189.

[6] Stanton, T. K., & Chu, D. (2008). Calibration of broadband active acoustic systems using a single standard spherical target. *J. Acoust. Soc. Am. , 124* (1), 128-136. [2] Foote, K. G. (1983). Maintaining precision calibrations with optimal copper spheres. *J. Acoust. Soc. Am. , 73* (3), 1054-1063.

[7] MacLennan, D. N., & Dunn, J. R. (1984). Estimation of sound velocities from resonance measurement on tungsten carbide calibration spheres. *Journal of Sound and Vibration , 97* (2), 321-331.

[8] Foote, K.G. (2007). Acoustic robustness of two standard spheres for calibrating a broadband multibeam sonar. *Oceans 2007 IEEE Conference Proceedings* , (pp. 1-4).

[9] Ona, E., Andersen, L.N., Knudsen, H.P., Berg, S. (2007). Calibrating multibeam, wideband sonar with reference targets. *Oceans 2007 IEEE Conference Proceedings* , (pp. 4-9).

[10] Lavery, A. C., Chu, D., & Moum, J. N. (2010). Measurements of acoustic scattering from zooplankton and oceanic microstructure using a broadband echosounder. *ICES Journal of Marine Science , 67* (2), 379-394.

[11] Tesei, A., Guerrini, P., & Zampolli, M. (2008). Tank measurements of scattering from a resin-filled fiberglass spherical shell with internal flaws. *J. Acoust. Soc. Am. , 124* (2), 827-840.

[12] Imaizumi, T., Furusawa, M., Akamatsu, T., & Nishimori, Y. (2008). Measuring the target strength spectra of fish using dolphin-like short broadband sonar signals. *J. Acoust. Soc. Am. , 124* (6), 3440-3449.

[13] Zhang, H., Chimenti, D. E., & Zeroug, S. (1998). Transducer misalignment effects in beam reflection from elastic structures. *J. Acoust. Soc. Am. , 104* (4), 1982-1991.

[14] Neubauer, W. G., Vogt, R. H., & Dragonette, L. R. (1974). Acoustic reflection from elastic spheres. I. Steady-state signals. *J. Acoust. Soc. Am. , 55* (6), 1123-1129.

[15] Bamber, J., & Phelps, J. (1977). The effective directivity characteristic of a pulsed ultrasound transducer and its measurement by semi-automatic means. *Ultrasonics* , 169-174.

[16] Vagle, S., Foote, K.G., Trevorrow, Mark V. and David M. Farmer (1996). A technique for calibration of monostatic echosounder sys tems. *IEEE J. Oceanic Eng.,* 298-305.

[17] Jech,M.J.,Chu, D.,Foote, K.G., Hammar,Terence R.,Hufnagle Jr., L.C. (2003). Calibrating two scientific echosounders. *Oceans 2003 MTS/IEEE Conference Proceedings* , (pp. 1625-1629).

[18] Foote, K.G., Chu, Dezhang, Hammar, T. R. Baldwin, K. C., Mayer, L.A., Hufnagle, Jr., L.C., Jech, M.J. (2005). Protocols for calibrating multibeam sonar. *J. Acoust. Soc. Am. , 117* (4), 2013-2027.

[19] Goodman, R. R., & Stern, R. (1962). Reflection and transmission of sound by elastic spherical shells. *J. Acoust. Soc. Am. , 34* (3), 338-344.

[20] Hampton, L. D., & McKinney, C. M. (1961). Experimental study of the scattering of acoustic energy from solid metal spheres in water. *J. Acoust. Soc. Am. , 33* (5), 664-673.

[[21] MacLennan, D. (1981). *The theory of solid spheres as sonar calibration targets.*. Scottish Fisheries Research.

[22] MacLennan, D. (1982). *Target strength measurements on metal spheres.* Scottish Fisheries Research.

[23] Feuillade, C., Meredith, R., Chotiros, N., & Clay, C. (2002). Time domain investigation of transceiver functions using a known reference target. *J.Acoust.Soc.Am. , 112* (6), 2702-2712.

[24] Welsby, V. G., & Goddard, G. C. (1973). Underwater acoustic target strength of nets and thin plastic sheets. *Journal of Sound and Vibration , 28* (1), 139-149.

[25] McCutcheon, S. C., Martin, J. L., & Barnwell, T. O. (1993). Handbook of hydrology. In D. R. Maidment, & D. R. Maidment (Ed.), *Handbook of hydrology.* New York: McGraw-Hill.

[26] Burdic, W. (1991). *Underwater acoustics system analysis* (2nd. ed.). Englewood Cliffs, New Jersey: Prentice-Hall.

[27] Miyanohana, Y., Ishii, K., & Furusawa, M. (1993). Spheres to calibrate echo sounders in any frequency. *NIppon Suisan Gakkaishi , 59* (6), 933-942.

[28] Del Grosso, V. (1974). New equation for the speed of sound in natural waters (with comparison to other equations). *J. Acoust. Soc. Am. , 56* (4), 1084-1091.

[29] Fofonoff, N. P., & Millard Jr., R. C. (1983). *Algorith for computation of fundamental properties of seawater.* Technical papers in marine science, UNESCO.

[30] Chen, C., & Millero, F. (1977). Sound speed in seawater at high pressures. *J. Acoust. Soc. Am. , 62*, 119-1135.

[31] Leroy, C. C., Robinson, S. P., & Goldsmith, M. J. (2008). A new equation for the accurate calculation of sound speed in all oceans. *J. Acoust. Soc. Am. , 124* (5), 2774-2782.

[32] Belogol'skii, V., Sekoyan, S. S., Samorukova, L., Stefanov, S., & Levtsov, V. (1999). Pressure dependence of the sound velocity in distilled water. *Meas. Tech. , 42*, 406-413.

[33] Chen, C., & Millero, F. (1977). The use and misuse of pure water PVT properties for lake waters. *Nature , 266*, 707-708.

[34] Chen, C., & Millero, F. (1986). Precise thermodynamic properties for natural waters covering only the limnological range. *Limnol. Oceanogr. , 31* (3), 657-662.

[35] Biernat Jr., S. (1995). Carbide coatability. *Cutting tool engineering , 47* (2).

[36] Aw, P.K., Kuan Tan, A.L., Tan, T.P., Qiu, J. (2008). Corrosion resistance of tungsten carbide based cermet coatings deposited by HighVelocity Oxy-Fuel spray process. *Thin Solid Films,* 516, 5710-5715.

[37] Gerlich, D., Kennedy, G.C. (1979). The elastic moduli and their pressure derivatives for tunsten carbide with different amounts of cobalt binder. *J. Appl. Phys.,* 50, 3331 - 3333.